Three-Level DTC-SVM with DC-Link Voltages Balancing Strategy of Double Star Induction Machine

Elakhdar Benyoussef[1] and Said Barkat[2]

[1]Faculty of Science Applied, Department of Electrical Engineering, University of Kasdi Merbah, Ouargla 30000, BP. 511, Algeria.
[2]Electrical Engineering Laboratory, Faculty of Technology, University of M'sila, M'sila 28000, BP. 166, Algeria.

Corresponding author: lakhdarbenyoussef@yahoo.com

Abstract: **This paper deals with direct torque control based on space vector modulation strategy of a double star induction machine supplied by two three-level diode-clamped inverters. This type of inverters has several advantages over the standard two-level inverter, such as lower voltage stress on power switches and less harmonic distortion in voltage and current waveforms. However, a very important issue in using a diode clamped inverter is the ability to guarantee the stability of the DC-link capacitors voltages. This drawback can be solved in satisfactory way by using multilevel space vector modulation technique equipped by a balancing strategy. Simulations results are given to show the effectiveness of the proposed control approach**.

Key words: **Double Star Induction Machine; Three-Level Inverter; Direct Torque Control; Space Vector Modulation; DC-voltages balancing strategy.**

1. Introduction

For many years, electrical drives are founded on the traditional three-phase machines. However, when enhancing power capabilities of the drive is considered, multiphase machine drives are potentially recommended. In fact, multiphase drives are useful for large systems such as naval electric propulsions systems, locomotive traction and electrical vehicles applications [1, 2].

A multiphase drive has more than three phases in the stator and the same number of inverter legs is in the inverter side. The main advantages of multiphase drives over conventional three-phase drives include increasing the inverter output power, reducing the amplitude of torque ripple and lowering the DC-link current harmonics [3].

One way to perform multiphase machines is to use double star technology. Indeed, in double star machine two sets of three-phase windings spatially phase shifted by 30 electrical degrees are implemented in the same stator. Two common examples of such structures are the double star synchronous machine and double star induction machine (DSIM) [4].

Normally two two-level inverters are indispensable for double star electrical drives. However, for high power applications multilevel inverters are often required. Many multilevel topologies have been developed [5], among them, the diode-clamped topologies (DCI), which can reach high output voltage, and high power levels with higher reliability due to its modular topology [6]. However, the unbalance of the input DC voltages constitutes the major limitation facing the use of this kind of power converter. Several methods are proposed to suppress the unbalance of DC-link capacitors voltages. Some of these methods are based on adding a zero sequence or a DC-offset to the output voltage [7]. Addition of auxiliary power electronics circuitry is another solution used to redistribute charges between capacitors [8]. SVM based DC capacitors voltages balancing method, which exploits the switching vectors redundancy to mitigate DC capacitors voltages drift, is one of the prominent solutions proposed in the literature to face this type of issues [9].

The multilevel direct torque control (DTC) of the multiphase machine has become an attracting topic in research and academic community over the past decade. This control is characterized by its good dynamic performances and robustness, because it requires no current regulators, no coordinate transformation and depends only on stator resistance [10]. This drives control utilizing hysteresis comparators suffers from high torque ripple and variable switching frequency. One common solution to those problems is to use the space vector modulation [11].

In this paper, a multilevel DTC-SVM with balancing strategy based on the switching states redundancy is proposed in order not only to improve the DSIM based drive performance but also to balance the DC-link capacitors voltages.

The remainder of this paper is structured as follows: in Section 2, the DTC-SVM with voltage balancing strategy scheme is presented. The model of the DSIM is presented in section 3; a suitable transformation matrix is used to develop a simple dynamic model. The proposed three-level DCI is presented in section 4. Section 5 is reserved to DC capacitor voltages balancing strategy. The DTC-SVM strategy is presented in section 6. The advantages of the proposed control system are shown by simulation results in section 7.

2. Structure of the Proposed Multilevel DTC-SVM Equipped by a Voltage Balancing Strategy

The general structure of the double star induction machine fed by two three-level inverters and controlled by direct

torque control based on space vector modulation with balancing strategy is represented in Fig. 1.

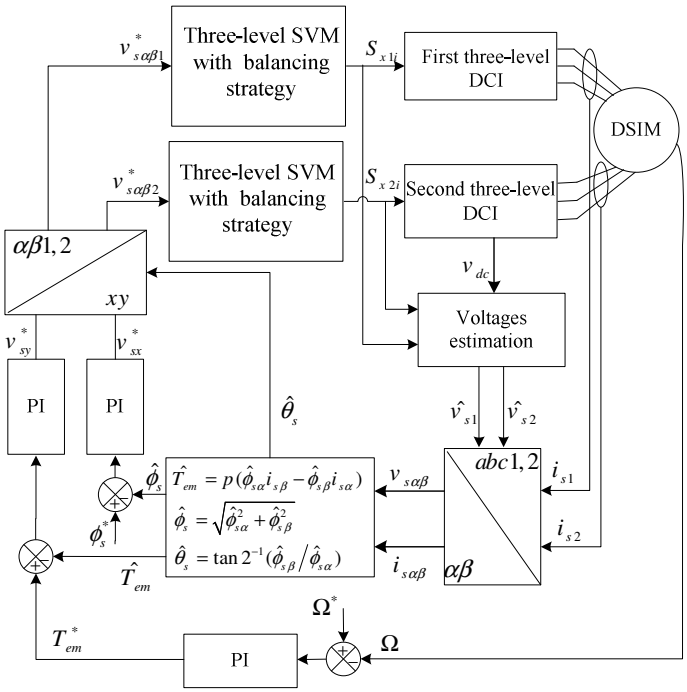

Fig. 1. DTC-SVM with balancing strategy of DSIM (with *i=1, 2, 3, 4*).

3. Double Star Induction Machine Modeling

The stator voltage equations can be expressed as:

$$\begin{bmatrix} v_{sa1} \\ v_{sb1} \\ v_{sc1} \\ v_{sa2} \\ v_{sb2} \\ v_{sc2} \end{bmatrix} = \begin{bmatrix} R_s & 0 & 0 & 0 & 0 & 0 \\ 0 & R_s & 0 & 0 & 0 & 0 \\ 0 & 0 & R_s & 0 & 0 & 0 \\ 0 & 0 & 0 & R_s & 0 & 0 \\ 0 & 0 & 0 & 0 & R_s & 0 \\ 0 & 0 & 0 & 0 & 0 & R_s \end{bmatrix} \begin{bmatrix} i_{sa1} \\ i_{sb1} \\ i_{sc1} \\ i_{sa2} \\ i_{sb2} \\ i_{sc2} \end{bmatrix} + \frac{d}{dt} \begin{bmatrix} \phi_{sa1} \\ \phi_{sb1} \\ \phi_{sc1} \\ \phi_{sa2} \\ \phi_{sb2} \\ \phi_{sc2} \end{bmatrix} \quad (1)$$

The rotor voltage equations can be expressed as:

$$\begin{bmatrix} 0 \\ 0 \\ 0 \end{bmatrix} = \begin{bmatrix} R_r & 0 & 0 \\ 0 & R_r & 0 \\ 0 & 0 & R_r \end{bmatrix} \begin{bmatrix} i_{ra} \\ i_{rb} \\ i_{rc} \end{bmatrix} + \frac{d}{dt} \begin{bmatrix} \phi_{ra} \\ \phi_{rb} \\ \phi_{rc} \end{bmatrix} \quad (2)$$

with

v_{sa1}, v_{sb1}, v_{sc1} : Stator voltages of the first winding;
v_{sa2}, v_{sb2}, v_{sc2} : Stator voltages of the second winding;
i_{sa1}, i_{sb1}, i_{sc1} : Stator currents of the first winding;
i_{sa2}, i_{sb2}, i_{sc2} : Stator currents of the second winding;
i_{ra}, i_{rb}, i_{rc} : Rotor currents;
ϕ_{sa1}, ϕ_{sb1}, ϕ_{sc1} : Stator flux of the first winding;
ϕ_{sa2}, ϕ_{sb2}, ϕ_{sc2} : Stator flux of the second winding;
ϕ_{ra}, ϕ_{rb}, ϕ_{rc} : Rotor flux;

The DSIM stator voltage equation (1) can decomposed into three subsystems (α,β), (z_1,z_2) and (z_3,z_4), using the following transformation:

$$\begin{bmatrix} X_{s\alpha} & X_{s\beta} & X_{z1} & X_{z2} & X_{z3} & X_{z4} \end{bmatrix}^T = [A][X_s] \quad (3)$$

with

$$[X_s] = [X_{s1} \quad X_{s2}]^T = [X_{sa1} \quad X_{sb1} \quad X_{sc1} \quad X_{sa2} \quad X_{sb2} \quad X_{sc2}]^T$$

where X_s can refer to stator currents vector, stator flux vector, or stator voltages vector.

The matrix A is given by:

$$[A] = \frac{1}{\sqrt{3}} \begin{bmatrix} \cos(0) & \cos\left(\frac{2\pi}{3}\right) & \cos\left(\frac{4\pi}{3}\right) & \cos(\gamma) & \cos\left(\frac{2\pi}{3}+\gamma\right) & \cos\left(\frac{4\pi}{3}+\gamma\right) \\ \sin(0) & \sin\left(\frac{2\pi}{3}\right) & \sin\left(\frac{4\pi}{3}\right) & \sin(\gamma) & \sin\left(\frac{2\pi}{3}+\gamma\right) & \sin\left(\frac{4\pi}{3}+\gamma\right) \\ \cos(0) & \cos\left(\frac{4\pi}{3}\right) & \cos\left(\frac{2\pi}{3}\right) & \cos(\pi-\gamma) & \cos\left(\frac{\pi}{3}-\gamma\right) & \cos\left(\frac{5\pi}{3}-\gamma\right) \\ \sin(0) & \sin\left(\frac{4\pi}{3}\right) & \sin\left(\frac{2\pi}{3}\right) & \sin(\pi-\gamma) & \sin\left(\frac{\pi}{3}-\gamma\right) & \sin\left(\frac{5\pi}{3}-\gamma\right) \\ 1 & 1 & 1 & 0 & 0 & 0 \\ 0 & 0 & 0 & 1 & 1 & 1 \end{bmatrix} \quad (4)$$

The voltage stator and rotor equations in stationary reference frame can be expressed as:

$$\begin{cases} v_{s\alpha} = R_s i_{s\alpha} + \dfrac{d\phi_{s\alpha}}{dt} \\ v_{s\beta} = R_s i_{s\beta} + \dfrac{d\phi_{s\beta}}{dt} \end{cases} \quad (5)$$

with

$v_{s\alpha}$, $v_{s\beta}$: The α-β components of stator voltage;
$i_{s\alpha}$, $i_{s\beta}$: The α-β components of stator current;
$\phi_{s\alpha}$, $\phi_{s\beta}$: The α-β components of stator flux;

The stator voltage equations in the stator flux reference frame are given by:

$$\begin{cases} v_{sx} = R_s i_{sx} + \dfrac{d\phi_{sx}}{dt} - p\Omega\phi_{sy} \\ v_{sy} = R_s i_{sy} + \dfrac{d\phi_{sy}}{dt} + p\Omega\phi_{sx} \end{cases} \quad (6)$$

with

v_{sx}, v_{sy}: The *x*-*y* components of stator voltage;
i_{sx}, i_{sy} : The *x*-*y* components of stator current;
ϕ_{sx}, ϕ_{sy}: The *x*-*y* components of stator flux;

The electromagnetic torque generated by the DSIM is:

$$T_{em} = p\left(\phi_{sx} i_{sy} - \phi_{sy} i_{sx}\right) \quad (7)$$

4. Three-Level DCI Modelling

The structure of a three-level diode-clamped inverter is shown in Fig. 2. Each leg is composed of two upper and lower switches with anti-parallel diodes. Two series DC-link capacitors split the DC-bus voltage in half, and six clamping

diodes confine the voltage across the switches within the voltage of the capacitors, each leg of the inverter can have three possible switching states; *2*, *1* or *0* [7].

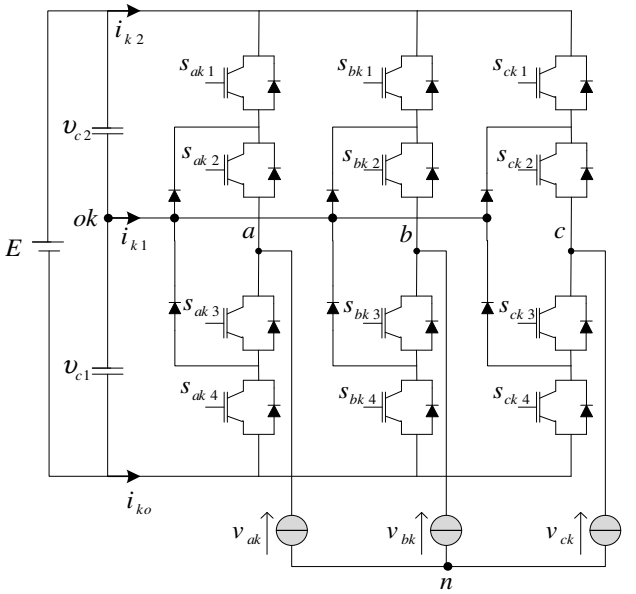

Fig. 2. Three-level DCI (*k*=1 for the first inverter and *k*=2 for the second inverter).

Functions of connection are given by:

$$\begin{cases} F_{xk2} = s_{xk1} s_{xk2}, \quad x = a,b,c \\ F_{xk1} = s_{xk3} s_{xk2} \end{cases} \tag{8}$$

The phase voltages v_{ak}, v_{bk}, v_{ck} can be written as:

$$\begin{bmatrix} v_{ak} \\ v_{bk} \\ v_{ck} \end{bmatrix} = \begin{bmatrix} 2F_{ak2}-F_{bk2}-F_{ck2} & 2F_{ak1}-F_{bk1}-F_{ck1} \\ 2F_{bk2}-F_{ak2}-F_{ck2} & 2F_{bk1}-F_{ak1}-F_{ck1} \\ 2F_{ck2}-F_{ak2}-F_{bk2} & 2F_{ck1}-F_{ak1}-F_{bk1} \end{bmatrix} \begin{bmatrix} v_{c1}+v_{c2} \\ v_{c1} \end{bmatrix} \tag{9}$$

The space vector diagram of a three-level inverter is showed in Fig. 3. The 27 switching states of three levels inverter corresponds to 19 different space vectors. These vectors have different effects on neutral point voltage variations [7].

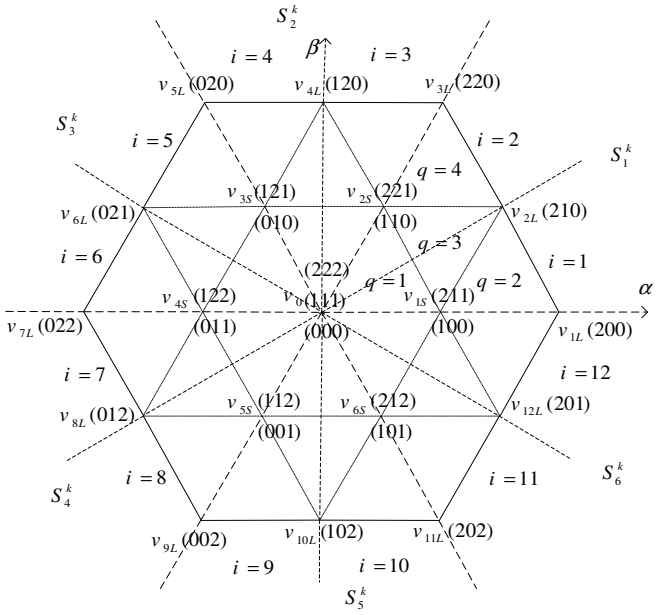

Fig. 3. Space vector diagram showing switching states for the three-level DCI.

In order to simplify three-level SVM algorithm, the reference voltage vector is only synthesized by the three basic voltage vectors within the minimum equilateral triangular area in which the reference voltage vector is located.

- Determination of the sector numbers

The reference vector magnitude and its angle are determined from:

$$\begin{cases} u_{refk} = \sqrt{u_{ref\,\alpha k}^2 + u_{ref\,\beta k}^2} \\ \vartheta_k = \tan 2^{-1}\left(\dfrac{u_{ref\,\beta k}}{u_{ref\,\alpha k}}\right) \end{cases} \tag{10}$$

The sector numbers *1-6* is given by:

$$S_n^k = ceil\left(\frac{\vartheta_k}{\pi/3}\right) \in \{1,\ 2,\ 3,\ 4,\ 5,\ 6\} \tag{11}$$

where ceil is the C-function that adjusts any real number to the nearest, but higher, integer [e.g. ceil (3.1) =4], (*n=1,…, 6*).

- Identification of the triangles

The reference vector is projected on the two axes making 60° between them. In each sector S_n^k, its components $u_{refk1}^{S_n^k}$ and $u_{refk2}^{S_n^k}$ are given by:

$$\begin{aligned} u_{refk1}^{S_n^k} &= 2M_k\left(\cos(\vartheta_k - (S_n^k - 1)\frac{\pi}{3}) - \frac{1}{\sqrt{3}}\sin(\vartheta_k - (S_n^k - 1)\frac{\pi}{3})\right) \\ u_{refk2}^{S_n^k} &= 2M_k\left(\frac{2}{\sqrt{3}}\sin(\vartheta_k - (S_n^k - 1)\frac{\pi}{3})\right) \end{aligned} \tag{12}$$

The modulation factor M_k is given by:

$$M_k = \frac{u_{refk}}{v_{dc}\sqrt{2/3}} \tag{13}$$

In order to determine the number of the triangle in a sector S_n^k, the two following numbers are to be defined:

$$\begin{aligned} l_{k1}^{S_n^k} &= \text{int}(u_{refk1}^{S_n^k}) \\ l_{k2}^{S_n^k} &= \text{int}(u_{refk2}^{S_n^k}) \end{aligned} \tag{14}$$

where *int* is a function which gives the whole part of a given real number.

Fig. 4 presents the projection of u_{refk} in the first sector.

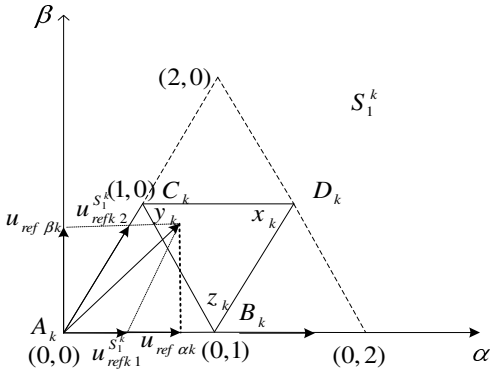

Fig. 4. First sector corresponding to the space voltage vectors of a three-level inverter.

In a reference frame formed by the two vectors $u_{refk\,1}^{S_n^k}$ and $u_{refk\,2}^{S_n^k}$ the coordinates of the tops A_k, B_k, C_k and D_k are given by:

$$\begin{aligned}
&\left(u_{A_{k1}}^{\Delta_q^{S_n^k}},\ u_{A_{k2}}^{\Delta_q^{S_n^k}}\right)=\left(l_{k1}^{S_n^k},\ l_{k2}^{S_n^k}\right)\\
&\left(u_{B_{k1}}^{\Delta_q^{S_n^k}},\ u_{B_{k2}}^{\Delta_q^{S_n^k}}\right)=\left(l_{k1}^{S_n^k}+1,\ l_{k2}^{S_n^k}\right)\\
&\left(u_{C_{k1}}^{\Delta_q^{S_n^k}},\ u_{C_{k2}}^{\Delta_q^{S_n^k}}\right)=\left(l_{k1}^{S_n^k},\ l_{k2}^{S_n^k}+1\right)\\
&\left(u_{D_{k1}}^{\Delta_q^{S_n^k}},\ u_{D_{k2}}^{\Delta_q^{S_n^k}}\right)=\left(l_{k1}^{S_n^k}+1,\ l_{k2}^{S_n^k}+1\right)
\end{aligned} \tag{15}$$

The following criteria (16) and (17) determine if the reference vector is located in the triangle formed by the tops A_k, B_k and C_k or in that formed by the tops B_k, C_k and D_k.

u_{refk} is in the triangle $A_kB_kC_k$ if:

$$u_{refk\,1}^{S_n^k}+u_{refk\,2}^{S_n^k}<l_{k1}^{S_n^k}+l_{k2}^{S_n^k}+1 \tag{16}$$

u_{refk} is in the triangle $B_kC_kD_k$ if:

$$u_{refk\,1}^{S_n^k}+u_{refk\,2}^{S_n^k}\geq l_{k1}^{S_n^k}+l_{k2}^{S_n^k}+1 \tag{17}$$

- *Calculation of application times*

If tops x_k, y_k, z_k corresponding has A_k, B_k, C_k, respectively, the application times are calculated by:

$$\begin{aligned}
t_{y_k}^{\Delta_q^{S_n^k}}&=\left(u_{refk\,1}^{S_n^k}-l_{k1}^{S_n^k}\right)T_s\\
t_{z_k}^{\Delta_q^{S_n^k}}&=\left(u_{refk\,2}^{S_n^k}-l_{k2}^{S_n^k}\right)T_s\\
t_{x_k}^{\Delta_q^{S_n^k}}&=T_s-\left(t_{yk}^{\Delta_q^{S_n^k}}-t_{zk}^{\Delta_q^{S_n^k}}\right)
\end{aligned} \tag{18}$$

where $t_{x_k}^{\Delta_q^{S_n^k}}, t_{y_k}^{\Delta_q^{S_n^k}}, t_{z_k}^{\Delta_q^{S_n^k}}$ are the application times of the vectors $u_{x_k}^{\Delta_q^{S_n^k}}, u_{y_k}^{\Delta_q^{S_n^k}}, u_{z_k}^{\Delta_q^{S_n^k}}$, respectively;

x_k, y_k and z_k are the tops of A_k, B_k, C_k respectively, $q=1,\ldots,4$.

5. Voltage Balancing Approach

The total energy of the two condensers is given by:

$$W=\frac{1}{2}\sum_{y=1}^{2}C_y\,\upsilon_{cy}^2 \tag{19}$$

Based on appropriate selection of redundant vectors [4], W can be minimized (ideally reduced to zero) if the capacitor voltages are maintained at voltage reference values of $E/2$. Assuming that all capacitors are identical, $C_1=C_2=C$, the mathematical condition to minimize W is:

$$\frac{dW}{dt}=C\sum_{y=1}^{2}\Delta\upsilon_{cy}\frac{d\,\upsilon_{cy}}{dt}=\sum_{y=1}^{2}\Delta\upsilon_{cy}\,i_{cy} \tag{20}$$

where $\Delta\upsilon_{cy}$ is the voltage deviation of capacitor C_y, $\Delta\upsilon_{cy}=\upsilon_{cy}-(E/2)$ and i_{cy} is the current through capacitor C_y. The capacitor currents i_{cy} in (20) are affected by the DC-side intermediate branch currents $i_{k\,2}$ and i_{k1}. These currents can be calculated if the switching states used in the switching pattern are known. Thus, it is advantageous to express (20) in terms of $i_{k\,2}$ and i_{k1}. The DC-capacitor current is expressed as:

$$i_{c\,2}=i_{c1}+\sum_{k=1}^{2}i_{k\,1} \tag{21}$$

Considering a constant DC-link voltage

$$\sum_{y=1}^{2}\Delta\upsilon_{cy}=0 \tag{22}$$

From (22) it is possible to deduced the following equation

$$\sum_{y=1}^{2}i_{cy}=0 \tag{23}$$

Solving (21) and (23), yields

$$i_{cy}=\frac{1}{2}\sum_{m=1}^{2}m\left(\sum_{k=1}^{2}i_{km}\right)-\sum_{m=y}^{2}\left(\sum_{k=1}^{2}i_{km}\right) \tag{24}$$

where $m=1, 2$.

By substituting i_{cy} into (20), the following condition to achieve voltage balancing is deduced:

$$\sum_{y=1}^{2}\Delta\upsilon_{cy}\left(\frac{1}{2}\sum_{m=1}^{2}m\left(\sum_{k=1}^{2}i_{km}\right)-\sum_{m=y}^{2}\left(\sum_{k=1}^{2}i_{km}\right)\right)\leq 0 \tag{25}$$

By substituting $\Delta\upsilon_{c\,2}$, calculated from (23), in (25) it yields

$$\Delta \upsilon_{c1}\left(\sum_{k=1}^{2} i_{k1}\right) \geq 0 \tag{26}$$

Applying the averaging operator, over one sampling period, to (26) results in:

$$\frac{1}{T}\int_{KT}^{(K+1)T} \Delta \upsilon_{c1}\left(\sum_{k=1}^{2} i_{k1}\right) dt \geq 0 \tag{27}$$

Assuming that the capacitor voltages can be assumed as constant values over one sampling period and consequently (27) is simplified to:

$$\Delta \upsilon_{c1}(K)\left(\frac{1}{T}\int_{KT}^{(K+1)T}\left(\sum_{k=1}^{2} i_{k1}\right)\right) dt \geq 0 \tag{28}$$

From (28), the final form of the cost function is given by:

$$W_k = \Delta \upsilon_{c1}(K)\left(\sum_{k=1}^{2} \bar{i}_{k1}(K)\right) dt \tag{29}$$

where $\Delta \upsilon_{c1}(K)$ is the voltage drift of C_1 at sampling period K, and $\bar{i}_{k1}(K)$ is the averaged value of the first DC-side intermediate branch current. Current $\bar{i}_{k1}(K)$ should be computed for different combinations of adjacent redundant switching states over a sampling period and the best combination which maximizes (29) is selected. If the reference vector is in the triangle $\Delta_q^{S_n^k}$ ($i=1,\ldots,6$, $q=1,..,4$), and $t_{x_k}^{\Delta_q^{S_n^k}}, t_{y_k}^{\Delta_q^{S_n^k}}, t_{z_k}^{\Delta_q^{S_n^k}}$ are the vectors application times presented in figure 2, the current $\bar{i}_{k1}^{S_n^k}$ is expressed by:

$$\bar{i}_{k1}^{S_n^k} = \frac{1}{T}\left[i_{1x_k}^{S_n^k} \quad i_{1y_k}^{S_n^k} \quad i_{1z_k}^{S_n^k} \right]\left[t_{x_k}^{\Delta_q^{S_n^k}} \quad t_{y_k}^{\Delta_q^{S_n^k}} \quad t_{z_k}^{\Delta_q^{S_n^k}} \right]^T \tag{30}$$

where $i_{1x_k}^{S_n^k}, i_{1y_k}^{S_n^k}$ and $i_{1z_k}^{S_n^k}$ are the charging currents to the states of commutation x_k, y_k and z_k in the triangle $\Delta_q^{S_n^k}$ minimizing the cost function W.

6. Direct Torque Control Based on Space Vector Modulation

The main idea behind the DTC-SVM control strategy is to force the torque and stator flux to follow their references by applying in one switching period several voltage vectors. This control algorithm uses prefixed time intervals within a cycle period and in this way a higher number of voltage space vectors can be synthesized with respect to those used in basic DTC technique [11].

The stator voltage can be estimated using equation (31) as follows:

$$\begin{bmatrix} \hat{v}_{s\alpha} \\ \hat{v}_{s\beta} \end{bmatrix} = [A]\begin{bmatrix} \hat{v}_{s1} \\ \hat{v}_{s2} \end{bmatrix} \tag{31}$$

with $\hat{v}_{s1} = [\hat{v}_{sa1} \quad \hat{v}_{sb1} \quad \hat{v}_{sc1}]$, $\hat{v}_{s2} = [\hat{v}_{sa2} \quad \hat{v}_{sb2} \quad \hat{v}_{sc2}]$

The presented control strategy is based on simplified stator voltage equations described in stator flux oriented x-y coordinates. The rotation transformation (32) transforms command variables in stator flux reference frame x-y to the stationary reference α-β :

$$\begin{bmatrix} v_{s\alpha 1}^* \\ v_{s\beta 1}^* \end{bmatrix} = [P(\theta_s)]\begin{bmatrix} v_{sx}^* \\ v_{sy}^* \end{bmatrix}, \quad \begin{bmatrix} v_{s\alpha 2}^* \\ v_{s\beta 2}^* \end{bmatrix} = [P(\theta_s - \gamma)]\begin{bmatrix} v_{sx}^* \\ v_{sy}^* \end{bmatrix} \tag{32}$$

with

$$[P(\theta_s)] = \begin{bmatrix} \cos(\theta_s) & -\sin(\theta_s) \\ \sin(\theta_s) & \cos(\theta_s) \end{bmatrix}$$

Since the stator flux is along the x-axis, it results in $\phi_{sy} = 0$ and $\phi_{sx} = \phi_s$. The presented control strategy is based on simplified stator voltage equations described in stator flux oriented x-y coordinates:

The stator voltage equations in x-y frame are:

$$\begin{cases} v_{sx} = R_s i_{sx} + \dfrac{d\phi_s}{dt} \\ v_{sy} = R_s i_{sy} + \omega_s \phi_s \end{cases} \tag{15}$$

The torque expression is simplified to:

$$\hat{T}_{em} = p\left|\hat{\phi}_s\right| i_{sy} \tag{16}$$

7. Simulation results

To verify the validity of the proposed controller, the system was simulated using the DSIM parameters given in Appendix. The DC side of the inverter is supplied by a constant source *600V*. The simulation results are obtained using the following DC-link capacitors values $C_1 = C_2 =$ *1*mF.

The obtained results are presented in Figs. 5 and 6 for the DTC-SVM without balancing strategy and that with balancing strategy, respectively. The DSIM is accelerated from standstill to reference speed *100* rad/s. The drive is simulated with load torque (T_L=*10*N.m), afterwards a step variation in the rated load (T_L = -*10*N.m) as well as a speed inversion from 100rad/s to -100rad/s are introduced at *0.8*s.

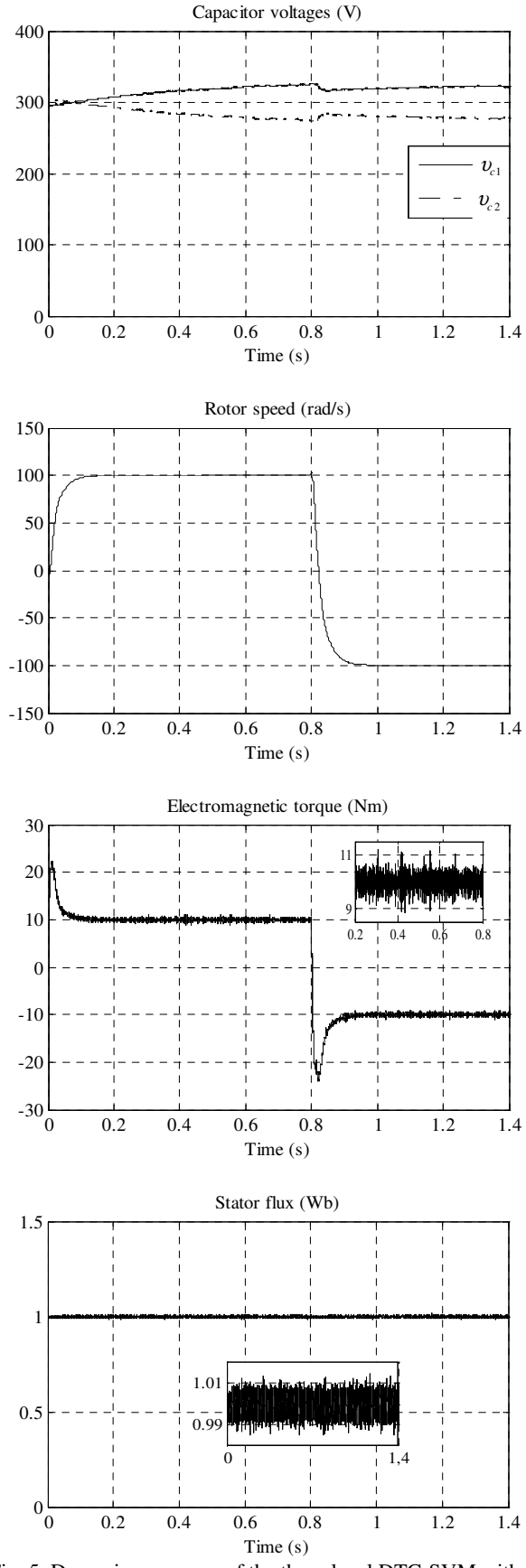

Fig. 5. Dynamic responses of the three-level DTC-SVM without balancing strategy for DSIM.

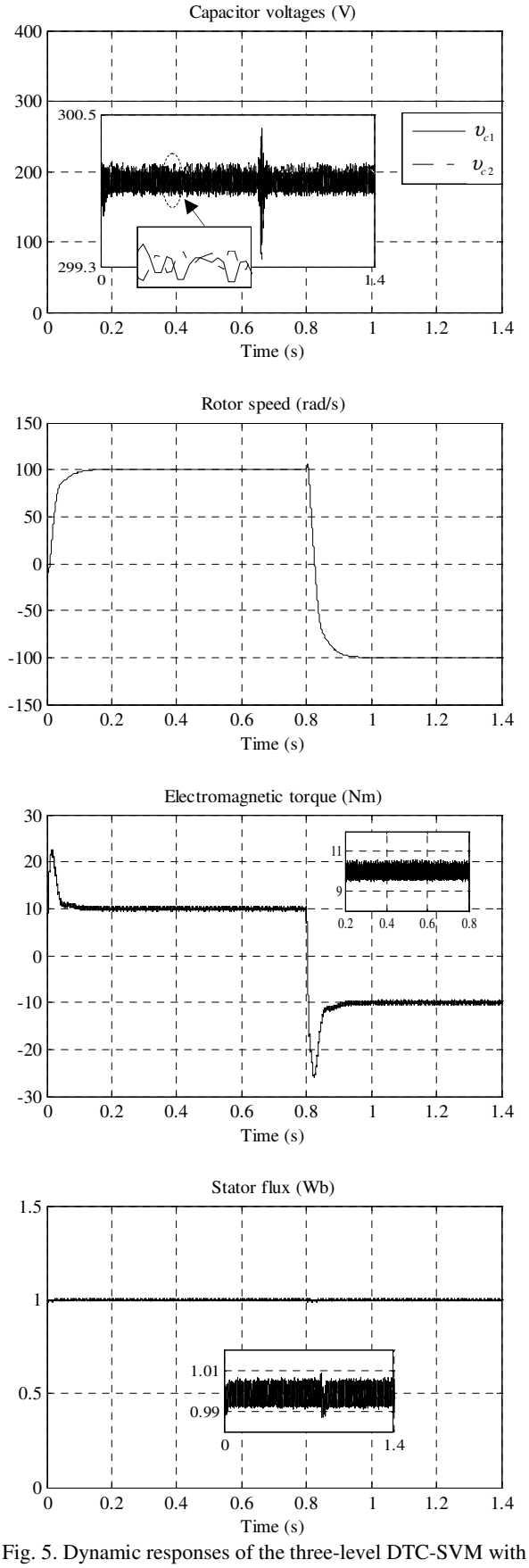

Fig. 5. Dynamic responses of the three-level DTC-SVM with balancing strategy for DSIM.

Note that the both proposed controls schemes present an excellent performance in terms of starting, rejection of disturbance and speed tracking. Also, the decoupling between the stator flux and electromagnetic torque is maintained in both configurations, confirming the good dynamic performances of the developed multiphase drive systems.

Referring to Fig. 5, it appears that the capacitor voltages given by v_{c1} and v_{c2} are deviating from their reference voltage value ($v_{dc}/2$). This result shows the problem of the unbalance capacitor voltages and its consequence on electromagnetic torque and stator flux harmonics rate. In order to improve the performance of the previous system, a three-level DTC-SVM based on balancing mechanism is proposed.

As expected in Fig. 6, the proposed solution is very efficient to solve the above-mentioned instability problem. As result, each capacitor voltage merged with its reference voltage value. Consequently, the torque and flux ripples decreases considerably using the proposed balancing strategy.

8. Conclusion

In this paper, an effective three-level DTC-SVM of DSIM is presented. The idea behind this control method is to gather the merits of the well-known DTC and those of the SVM equipped by a balancing strategy in the aim to improve the performance of the overall multiphase drive.

From the obtained simulation results, it is pointed out that the robustness of the controlled DSIM drive against speed and load torque variations is guaranteed. On the other hand, to take full benefit of multilevel DCI inverter, the proposed control method is endowed by a suitable balancing strategy able to ensure the stability of DC-link capacitor voltages. The simulation results confirm that the proposed direct torque control based on space vector modulation scheme with balancing strategy achieves a fast electromagnetic torque response with low torque ripples, in comparison to that control scheme without balancing strategy. Moreover, it performs well under various condition variations such as sudden change in the speed reference, speed reversion operation, and step change of the load torque.

Declaration of conflicting interest

This work was supported by the Directorate-General for Scientific Research and Technological Development (DG-RSDT) of Algeria under PRFU project number A01L07UN300120200001.

9. Appendix

The parameters of DSIM are given in Table 1.

Table 1. DSIM parameters.

1kW, 2 Poles, 220 V, 50 Hz		
Quantity	Symbol	Value
Stator resistance	R_s	4.67 Ω
Rotor resistance	R_r	8 Ω
Stator inductance	L_s	0.374 H
Rotor inductance	L_r	0.374 H
Mutual inductance	M	0.365 H
Inertia moment	J	0.003 kgm^2

11. References

1. Levi E., "Multiphase Electric Machines for Variable-Speed Applications," IEEE Transactions on Industrial Electronics, Vol. 55, No. 5, 2008, pp. 1893-1909.
2. Riveros, B. Bogado, J. Prieto, F. Barrero, S. Toral, and M. Jones, "Multiphase Machines in Propulsion Drives of Electric Vehicles," International Power Electronics and Motion Control Conference, Ohrid, Macedonia, September 2010, pp. 201-206.
3. Abuishmais I., Arshad W., and Kanerva S., "Analysis of VSI-DTC Fed 6-phase Synchronous Machines," IEEE International Power Electronics and Motion Control Conference, December 2009, pp. 867-873.
4. Oudjebour Z., Berkouk E., and Mahmoudi M., "Stabilization by New Control Technique of the Input DC Voltages of five-level Diode-Clamped Inverters Application to Double Star Induction Machine," International Symposium on Environment-Friendly Energies and Applications, Newcastle upon Tyne, UK, 25-27 June 2012, pp. 541-544.
5. Singh B., Mittal N., Verma D., Singh D., Singh S., Dixit R., Singh M., and Baranwal A., "Multi-Level Inverter: a Literature Survey on Topologies and Control Strategies," International Journal of Reviews in Computing, Vol. 10, 2012, pp. 1-16.
6. Saeedifard M., Iravani R., and Pou J., "Control and DC-Capacitor Voltage Balancing of a Space Vector-Modulated Five-Level STATCOM," Institution of Engineering and Technology, IEEE Transaction on Energy Conversion, Vol. 2, No. 3, 2009. pp. 203-215.
7. Pan Z., Peng F., Corzine K., Stefanovic V., Leuthen j., and GataricS., "Voltage Balancing Control of Diode-Clamped Multilevel Rectifier/Inverter Systems," IEEE Transactions on Industry Applications, Vol. 41, No. 6, 2005, pp. 1698-1706.
8. Chibani R., Berkouk E., and Boucherit M., "Five-Level NPC VSI: Different Ways to Balance Input DC Link Voltages," Elektrika, Vol. 11, No. 1, 2009, pp. 19-33.
9. Saeedifard M., Iravani R., and Pou J., "Analysis and Control of DC-Capacitor-Voltage-Drift Phenomenon of a Passive Front-End Five-Level Converter," IEEE Transactions on Industrial Electronics, Vol. 54, No. 6, 2007, pp. 3255-3266.
10. Wenhao C., and jiangxia C., "Speed Identification Method in Direct Torque Control of Asynchronous Machine Based on Neuron Network Theory," IEEE, International Conference on Computer Application and System Modeling, Taiyuan, China, October 2010, pp. 133-136.
11. Hassankhan E., and Khaburi D., "DTC-SVM Scheme for Induction Motors Fed with a Three-level Inverter," World Academy of Science, Engineering and Technology, Vol. 44, 2008, pp. 168-172.